



Non-equilibrium molecular dynamics simulations of the spallation in Ni: Effect of vacancies



Tian Qiu^a, Yongnan Xiong^b, Shifang Xiao^a, Xiaofan Li^a, Wangyu Hu^b, Huiqiu Deng^{a,b,*}

^a Department of Applied Physics, School of Physics and Electronics, Hunan University, Changsha 410082, China

^b College of Materials Science and Engineering, Hunan University, Changsha 410082, China

ARTICLE INFO

Article history:

Received 30 January 2017

Received in revised form 24 May 2017

Accepted 25 May 2017

Keywords:

Spallation

Vacancy concentration

Shock wave

Molecular dynamics simulations

ABSTRACT

The effects of defects on the fracture resistance of materials have attracted considerable attention recently. In the present work, the vacancy effects on the spallation in single-crystalline Ni are studied by nonequilibrium molecular dynamics simulations. The vacancy concentration ranges from 0% to 2.0%, and the spallation in shock wave loading along three low-index directions ([001], [110], and [111]) is investigated. We found that vacancies provide the sites of nucleation for compression-induced plasticity, and tension stress-induced plasticity plays the key role in void nucleation. Along the [001] direction, the degree of spall damage does not increase with the increase in vacancy concentration; however, along the [110] and [111] directions, it decreases with the increase in vacancy concentration when the vacancy concentration is higher than the threshold value.

© 2017 Elsevier B.V. All rights reserved.

1. Introduction

Spallation is a typical phenomenon of dynamic fracture under shock wave loading [1–3], which is due to the interaction of the unloading incident waves and reflected waves. The mechanisms of spallation are dominated by nucleation, growth, and coalescence of voids or cavities produced by shock waves [4–6]. A deep understanding of spallation is of great help for the construction of dynamic failure models of materials.

Experimentally, a single-crystalline material is preferred for spall study because of it has a simple structure and can be easily analyzed [7–10]. Spall strength in aluminum and copper shocked by a high-power laser was measured, and a rapid increase in the spall strength with a strain rate about 10^7 s^{-1} was observed. The spall mechanism at low/high strain rates was discussed in the study [7]. By using a pulsed high-power laser, spallation in two ductile metals, namely tin and zinc, was studied. A highly accurate continuous measurement in time for obtaining the free surface velocity time history was proposed [9]. The effects of microstructure on the spall failure were studied for four aluminum materials by plate-impact spall experiments. Spall strength and void process in the four systems were discussed [10]. Void initiation and growth in Cu were revealed by laser shock experiments, and the

dislocation-emission-based mechanism for void growth was discussed in detail [11]. Thus, a comprehensive understanding of the spallation phenomenon, in addition to the spall strength and spall mechanism, was obtained from previous experimental studies. However, the effects of defect structure on spallation was mentioned in the abovementioned studies, which is also worthy of our attention. For example, the critical tension in the simulation was higher than the tension inferred from experiments on materials with natural defects [8]. It was found that the higher the purity of Al, the better is the resistance for void nucleation and the higher is the spall strength [10]. Vacancy defect is one of the most common defects. At ambient conditions, vacancy concentration is very low in thermal equilibrium [12], and its effects are expected to be negligible. However, materials with high vacancy concentration (c_v) can be achieved by rapid quenching, ion radiation, and thin film growth. For example, In 150-kbar, shock-loaded molybdenum wires, c_v of 1.2% and 2.2% were obtained by temperature annealing at 1250 °C [13]. The growth of Ag on Ag(001) and Ag(111) surfaces at $T = 100 \text{ K}$ was investigated, and it was found that a high c_v (2%) was observed in the evolving film during the growth [14]. Therefore, it is worthy to study the effects of high c_v on the damage resistance of materials. Spallation in Cu with c_v ranging from 0% to 2.0% was explored by Luo et al. [15]. They showed that the shear flow strength and the spall strength decrease with the increase in c_v . Lin et al. [16] extended their research to [110] and [111] directions and indicated the difference in shock loading along three

* Corresponding author at: Department of Applied Physics, School of Physics and Electronics, Hunan University, Changsha 410082, China.

E-mail address: hq Deng@hnu.edu.cn (H. Deng).

low-index crystal orientations for different c_v . They pointed out that the spall damage is not positively correlated with the c_v along the [110] and [111] directions.

As a typical FCC material, single-crystalline Ni has been extensively studied to determine their properties under dynamic loading [17–19], and a certain concentration of vacancies can be fixed in it upon the irradiations at the room temperature [20]. However, spallation in Ni with vacancies has not yet been studied. In this paper, nonequilibrium molecular dynamics (NEMD) simulations [21] are used to investigate the effects of c_v from 0% to 2% on spallation in single-crystalline Ni. Samples for shock loading along the [001], [110], and [111] directions are analyzed, respectively. We show the effects of c_v on shock Hugoniot response, free surface velocity history, and microstructures under compression and tension. Moreover, we analyze the different spall damages caused by different c_v values.

2. Modeling and simulation method

NEMD simulations are performed by the Large-scale Atomic/Molecular Massively Parallel Simulator (LAMMPS) code [22] and an embedded-atom method (EAM) interatomic potential for Ni [23]. To investigate the effect of crystal orientation on spallation, perfect single crystalline Ni samples are first prepared with the three coordinate axes (X, Y, and Z) along the ([100], [010], [001]), ($[\bar{1}10]$, [001], [110]) and ($[\bar{1}\bar{1}0]$, $[1\bar{1}\bar{2}]$, [111]) crystal directions, and they have a size of $17.6 \times 17.6 \times 141.0 \text{ nm}^3$, $17.6 \times 17.7 \times 149.5 \text{ nm}^3$ and $17.3 \times 17.9 \times 146.5 \text{ nm}^3$, respectively. Samples with initial c_v are achieved by randomly removing a certain percentage of atoms from the resulting configurations, where c_v ranges from 0% to 2.0%. The samples are then equilibrated for 100–200 ps at 300 K and zero pressure under the constant pressure–temperature (NPT) ensemble, and the three-dimensional (3D) periodic boundary conditions (PBC) are applied. After being quenched, the vacancy concentration remains approximately unchanged (despite a small decrease in the high vacancy concentration), and the randomly distributed vacancies remain predominantly as monovacancies, followed by divacancies, and only a few number of voids or larger vacancy clusters can be found, which is similar to that observed by Luo et al. [15].

During dynamic loading (along the z-axis), constant volume–energy (NVE) ensemble [24] is adopted. PBCs are imposed in the x and y directions, and free surfaces are adopted along the z direction. To better describe the process of spalling, the samples are divided into two parts: piston and target. The piston consists of several layers of atoms, while the rest is the target. When the moving infinite massive piston impacts the target at a certain piston velocity (V_p), compressive shock waves are initiated [25]. Upon reflection at the free surfaces, the compressive shock waves are transformed into tensile waves. Tensile stresses operate on the local area where unloading waves and reflected waves meet each other. Spallation will occur if the tensile strength is strong enough.

The time step for integrating the equations of motion is 1 fs. A binning analysis [26] is used to obtain the stress σ_{zz} ; particle velocity V_p ; and temperature and density profiles along the z-axis at three stages: compression, release, and tension. Stress tensor is obtained from the atomic virial. Temperature is calculated by subtracting the center-of-mass velocity from the average kinetic energy of each bin. The velocity of shock wave (V_s) can be measured from the shock front propagation at different time steps. The free surface velocity (V_{fs}) profile is obtained from the particle velocity evolution on the free surface of target at all time points. Adaptive common neighbor analysis (ACNA) [27] within OVITO [28] is used to analyze the crystal structures and local crystalline defects during the deformation simulations.

3. Results and discuss

3.1. Shock Hugoniot response

It is known that only an elastic wave can travel through the targets if the given loading strength is lower than the Hugoniot elastic limit (HEL) of a perfect single crystalline [15,29]. In the present work, the HEL of perfect single-crystalline Ni is about 40 GPa, corresponding to the piston velocity (V_{pHEL}) $\sim 0.7 \text{ km/s}$. When $V_p = 0.68 \text{ km/s}$ is applied to the piston, a single front shock wave propagates through the sample, as shown in Fig. 1(a). Because

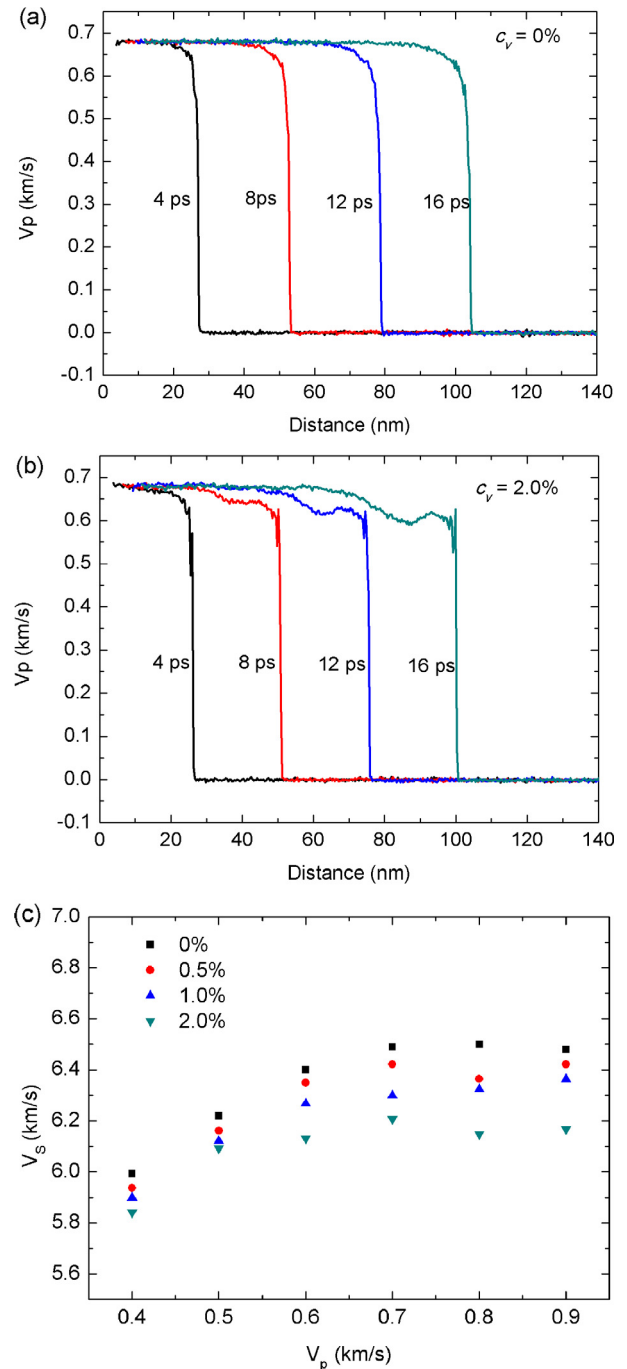


Fig. 1. Piston velocity profiles at 4, 8, 12, and 16 ps in the cases of (a) perfect crystal and (b) $c_v = 2\%$ for $V_p = 0.68 \text{ km/s}$; (c) V_s – V_p relationship for different vacancy concentrations.

Download English Version:

<https://daneshyari.com/en/article/5453385>

Download Persian Version:

<https://daneshyari.com/article/5453385>

[Daneshyari.com](https://daneshyari.com)